



Published in final edited form as:

Mol Cancer Ther. 2014 July ; 13(7): 1848–1859. doi:10.1158/1535-7163.MCT-13-0576.

Evaluation of Apoptosis Induction by Concomitant Inhibition of MEK, mTOR, and Bcl-2 in Human Acute Myeloid Leukemia Cells

Weiguo Zhang¹, Vivian R. Ruvolo¹, Chen Gao¹, Liran Zhou¹, William Bornmann³, Twee Tsao¹, Wendy D. Schober¹, Paul Smith⁴, Sylvie Guichard⁴, Marina Konopleva^{1,2}, and Michael Andreeff^{1,2}

¹Section of Molecular Hematology and Therapy, The University of Texas MD Anderson Cancer Center, Houston, Texas, U.S.A.

²Department of Leukemia, The University of Texas MD Anderson Cancer Center, Houston, Texas, U.S.A.

³Department of Experimental Therapeutics, The University of Texas MD Anderson Cancer Center, Houston, Texas, U.S.A.

⁴Oncology iMED, AstraZeneca, Alderley Park, Macclesfield SK10 4TG, UK

Abstract

Aberrant activation of multiple signaling pathways is common in acute myeloid leukemia (AML) cells, which can be linked to a poor prognosis for patients with this disease. Previous research with mTOR or MEK inhibitors revealed cytostatic, rather than cytotoxic, effects in *in vitro* and *in vivo* AML models. We evaluated the combination effect of the mTOR inhibitor AZD8055 and the MEK inhibitor selumetinib on human AML cell lines and primary AML samples. This combination demonstrated synergistic proapoptotic effects in AML cells with high basal activation of MEK and mTOR. We next incorporated the BH3 mimetic ABT-737 into this combination regimen to block Bcl-2, which further enhanced the apoptogenic effect of MEK/mTOR inhibition. The combination treatment also had a striking proapoptotic effect in CD33⁺/CD34⁺ AML progenitor cells from primary AML samples with *NRAS* mutations. Mechanistically, up-regulation of the proapoptotic protein Bim, accompanied by the down-regulation of the antiapoptotic protein Mcl-1 (mainly via protein degradation), appeared to play critical roles in enhancing the combination drug effect. Furthermore, the modulation of survivin, Bax, Puma, and XIAP expression suggested a role for mitochondria-mediated apoptosis in the cytotoxicity of the drug combination. Consequently, the concomitant blockade of pro-survival MEK/mTOR signaling and the deactivation of Bcl-2 could provide a mechanism-based integrated therapeutic strategy for the eradication of AML cells.

Keywords

AZD8055; selumetinib; ABT-737; acute myeloid leukemia; apoptosis

Corresponding Authors: Michael Andreeff (mandreeff@mdanderson.org) and Marina Konopleva (mkonople@mdanderson.org), The University of Texas M. D. Anderson Cancer Center, 1515 Holcombe Blvd., Unit 448, Houston, TX 77030, U.S.A..

The authors disclose no potential conflicts of interest.

Introduction

Aberrant gene expression/signaling pathways like the RAS/Raf/mitogen-activated protein kinase (MAPK) kinase (MEK)/extracellular-regulated kinase (ERK) and the phosphatidylinositol 3-kinase (PI3K)/Akt/mammalian target of rapamycin (mTOR) pathways can promote tumorigenesis in many tissues including the hematopoietic system. Indeed, the deregulation of RAS/Raf/MEK/ERK or PI3K/Akt/mTOR signaling has been shown to contribute to leukemogenesis (1-3), and the *NRAS*-activating mutations, which abnormally stimulate RAF/MEK/ERK and PI3K/AKT/mTOR, are found in about a third of hematopoietic malignancies including acute myeloid leukemia (AML) (1). Furthermore, we have previously reported that the simultaneous activation of the aforementioned signaling pathways is consistently associated with poor disease prognosis in patients with AML (4).

In several studies by our group and others, the MEK inhibitors CI1040 and selumetinib (also known as AZD6244) exerted mainly cytostatic effects in *in vitro* and *in vivo* AML models. This was also the case for the mTOR inhibitors CCI779 and RAD001 (5-7). Thus, interrupting one of these signaling pathways independently appears to be insufficient to trigger cell death in AML cells (5,8,9).

The B-cell lymphoma 2 (Bcl-2) family of proteins are key regulators of cancer cell apoptosis. The anti-apoptotic Bcl-2 proteins Bcl-2, Bcl-xL, and myeloid cell leukemia sequence 1 (Mcl-1) prevent cellular apoptosis via their expression and dimerization with the pro-apoptotic Bcl-2 proteins Bim and Bax. The overexpression of the anti-apoptotic Bcl-2 proteins correlates with an overall lower overall survival rates for AML patients (10,11). Several small-molecule Bcl-2 inhibitors have been developed, and they have shown encouraging single-agent activity in preclinical and clinical trials (12,13). We hypothesize that the concomitant blockade of the MAPK and mTOR signaling, in conjunction with interference with anti-apoptotic Bcl-2 family members, could promote marked cytotoxic activity in AML cells, including AML stem cells. The purpose of this study was to determine if, and by what mechanisms, the co-suppression of MEK and mTOR signaling in concert with the interruption of anti-apoptotic Bcl-2 family members could effectively induce apoptosis in AML cells. We examined a three-drug combination consisting of the mTOR inhibitor AZD8055, the MEK inhibitor selumetinib, and the anti-apoptotic Bcl-2 family mimetic ABT-737 on human AML cells and primary AML samples. This combination demonstrated marked pro-apoptotic effects in AML cells with high basal activation of MEK and mTOR. The rationale for this combination treatment was based on: 1) the ability to disable Mcl-1-mediated resistance associated with the inhibition of pERK, 2) overcoming resistance to MEK inhibition mediated by constitutive and reactive PI3K/AKT in AML cells (12,14), and 3) by mediating loss of mitochondrial inner transmembrane potential in the presence of Bcl-2 antagonist ABT-737. Our results suggest this drug combination can be potentially effective in eradicating AML cells, and, as such, could be an important strategy for controlling AML *in vivo*.

Materials and Methods

Reagents and antibodies

Selumetinib (also known as AZD6244 and ARRY-142886) and AZD8055 were provided by AstraZeneca (Macclesfield, UK). ABT-737 was synthesized at the University of Texas MD Anderson Cancer Center based on its published chemical structure (15). The chemical structures of the above-mentioned reagents are shown at Supplementary Figure S1. Antibodies against human phosphorylated (p)-p44/42 MAPK (ERK1/2)(Thr202/Tyr204), p-AKT(Ser473), p-AKT(Thr308), p-S6K(Ser240/244), p-Rb (Ser780), p-4E-BP1 (Thr37/46), p-Bad (Ser136), p-MEK1/2 were purchased from Cell Signaling Technology (Danvers, MA), as were the antibodies against AKT, S6K, 4E-BP1, Bad, Bid, Bcl-xL, survivin, caspase-8, caspase-9, and cleaved-caspase-3. Antibodies against Bax, Mcl-1, XIAP, and p27Kip-1 were purchased from BD Biosciences (San Jose, CA), antibody against Bcl-2 was purchased from Dako (Carpinteria, CA), antibody against Bak was purchased from Upstate (Lake Placid, NY), antibodies against ERK2, Cdk2, and Cdk4 were purchased from Santa Cruz Biotechnology (Santa Cruz, CA), and antibodies against Bim, cyclin D1, Cdc2, and Puma were purchased from CalBiochem (San Diego, CA).

AML cell lines and patient samples

The human AML cell lines U937, KG-1 and MV4-11 were obtained from the American Type Culture Collection (Manassas, VA). The OCI/AML3 cell line was kindly provided by Dr. M. Minden (Princess Margaret Hospital, Toronto, Ontario, Canada). The MOLM13 cell line was obtained from the Deutsche Sammlung von Mikroorganismen und Zellkulturen (Braunschweig, Germany). U937, KG-1, MOLM13, and OCI/AML3 cells were validated in September 2010 by short tandem repeat DNA fingerprinting using the AmpFISTR Identifier kit according to manufacturer's instructions (Applied Biosystems). Genetic characteristics of AML cell lines used in this study are summarized in Supplementary Table 1.

Peripheral blood and bone marrow samples were obtained from patients with newly diagnosed, relapsed, or refractory AML after written informed consent had been obtained from each patient according to institutional guidelines of the University of Texas, MD Anderson Cancer Center. All cells, including those obtained from peripheral blood and bone marrow samples, were cultured in RPMI 1640 culture medium supplemented with 10% fetal calf serum.

Cell viability and apoptosis assays

Cell viability was assessed using an automated cell counter employing the Trypan blue dye exclusion method, and cell apoptosis was examined by flow cytometry as described previously (16). To evaluate apoptosis induction by treatment with AZD8055 plus selumetinib in 2 sets of peripheral blood and bone marrow samples (with and without *NRAS* mutations), mononuclear cells were separated by Ficoll-Hypaque density-gradient centrifugation (Sigma Chemicals, St. Louis, MO, USA). Apoptosis of bulk leukemic and leukemic progenitor cells (i.e., gating the AML cells with CD34⁺ or CD33⁺) was determined as described above. Induction of specific apoptosis was calculated using the following

formula: specific apoptosis (%) = 100 (drug-induced apoptosis – spontaneous apoptosis)/ (100 – spontaneous apoptosis) (17).

Cell proliferation assay

AML cells were treated with the indicated agent for 24 hours, and bromodeoxyuridine (BrdU, BD Pharmingen) was added to the medium at the last 45 minutes of treatment to allow BrdU incorporation into newly synthesized cellular DNA. The cells were harvested and fixed in 70% cold ethanol, and BrdU was labeled with an anti-BrdU-fluorescein isothiocyanate antibody and measured using flow cytometry (18).

Immunoblot and immunoprecipitation analyses

AML cells were treated with AZD8055, selumetinib, or ABT-737 alone or in combination as indicated and then collected for analysis. Semi-quantitative immunoblotting data were generated using the Scion imaging software program (Beta version 4.03; Scion, Frederick, MD) (18).

For the immunoprecipitation studies, AML cells were lysed and the cell lysates (containing ~ 0.5 mg of total protein in each sample) were incubated overnight with a primary anti-Bcl-2 antibody. Protein A/G PLUS-agarose (Santa Cruz Biotechnology, Santa Cruz, CA) was added to the lysis buffer for an additional 4 hours of incubation at 4°C. Bcl-2 family proteins were resolved using sodium dodecyl sulfate-polyacrylamide gel electrophoresis. The amount of Bax bound to Bcl-2 was determined using immunoblotting analysis with an anti-Bax antibody.

Knock down of Bim or Mcl-1 protein

Bim protein was knocked down by transfecting small interfering RNAs (siRNAs, sequence: 5'-GACCGAGAAGGUAGACAAUUGdTdT-3) and mock control siRNAs (Dharmacon RNAi Technologies, Lafayette, CO) in to OCI/AML3 and U937 leukemia cells using an electroporation method (T-solution, X-001 and C-solution, W-001, respectively; Amaxa Biosystems, Gaithersburg, MD) following the manufacturer's instructions. The final concentration of siRNA in the electroporation buffer was 200 nM.

Mcl-1 protein was knocked down by lentiviral transfection with a gene-specific short hairpin RNA (shRNA) transfer vector targeting residues 2421–2440 on RefSeq NM_021960.4. Lentivirus was prepared by co-transfection of HEK293T cells (American Type Culture Collection) with an equal molar mix of transfer vector and packaging plasmids (psPAX2 and pMD2.G; plasmids 12260 and 12259, respectively, from Addgene, Cambridge, MA) using JetPrime transfection reagent as directed in the manufacturer's instructions (Polyplus, Illkirch, France). The OCI/AML3 cells underwent lentivirus transfection with Mcl-1 shRNA vector or nonspecific control vector (pLKO.1 TRC control, plasmid 10879, Addgene) and selected with puromycin (Invitrogen, San Diego, CA) starting at 0.5 µg/mL. Knockdown was verified by immunoblot analysis and real-time polymerase chain reaction (PCR).

Real-time PCR assays

The OCI/AML3 and MOLM13 cells were treated with the indicated drugs for 6 hours, and total RNA was extracted with Trizol (Life Technologies, Grand Island, NY) following the manufacturer's protocol. cDNA was synthesized as described previously (19), and duplicated TaqMan gene expression assays were carried out in a 25- μ L reaction containing the cDNA equivalent of 1.0 ng of total RNA with TaqMan gene expression assays (Life Technologies) for Mcl-1 (Hs03043899_m1), Bim (Hs00708019_s1), or housekeeping gene 18S (Hs03928985_g1) using an ABI model 7900HT fast real-time PCR system. Data were analyzed by the $\Delta\Delta$ Ct method using RQ Manager 1.2.1 software (Life Technologies) and the relative abundance of target in treated cells, normalized to that of vehicle treated cells, is reported as follows: $RQ = 2^{-\Delta\Delta Ct}$, where $\Delta\Delta Ct = \Delta Ct_{\text{treated}} - \Delta Ct_{\text{vehicle}}$, and $\Delta Ct = Ct_{\text{gene of interest}} - Ct_{18S}$.

Establishment of *NRAS*-mutated leukemia cells

A plasmid harboring the *NRAS* cDNA (IMAGE:3826638, Open Biosystems, Huntsville, AL) was used as a template to generate the *NRAS* open reading frame (ORF) flanked by *NheI* (5') and *XhoI* (3') sites by PCR with HiFi Hot Start polymerase (Kapa Biosystems, Woburn, MA) and the primers TGTGAAGCTAGCCGCCATGACTGAGTACAAACTGG (forward) and CCTCGAGTTACATCACACATGGCAATCCC (reverse). An expression vector with the *NRAS* cDNA was constructed by replacing the ORF for enhanced green fluorescent protein in EGFPc2 with the ORF for *NRAS* as a *NheI*-to-*XhoI* construction. This expression vector was used to generate the G12D mutant with a QuikChange II XL site-directed mutagenesis kit (Agilent Technologies, Santa Clara, CA) and the primers GTG GTG GTT GGA GCA GAT GGT GTT GGG AAA AGC GCA CTG AC (forward) and GTC AGT GCG CTT TTC CCA ACA CCA TCT GCT CCA ACC ACC AC (reverse). Lentiviral transfer vectors were then constructed by inserting the wild type or mutant G12D between the *NheI* and *NotI* sites of pCDH-CMV-MSC-EF1-Puro (System Biosciences, Mountain View, CA). The vectors were introduced into MV4-11 cells by lentiviral transduction as described (20). Positive cells were selected and maintained with puromycin (up to 1 g/mL). *NRAS* activation was confirmed by measuring the phosphorylation level of MEK by immunoblotting.

Mitochondrial inner transmembrane potential (Ψ_m) analysis

MV4-11-*NRAS*-WT and MV4-11-*NRAS*-mutated cells were treated with AZD8055, selumetinib, or ABT-737 alone or in combination as indicated for 24 hours and then collected for staining with CMXRos (300 nmol/L) and MitoTracker Green (100 mol/L) (both from Molecular Probes, Eugene, OR) for 1 hour at 37°C. The Ψ_m was determined using flow cytometry by measuring CMXRos retention (red fluorescence) while simultaneously adjusting for the mitochondrial mass (green fluorescence as described previously (21)).

Statistical analyses

The Student *t*-test was used to analyze immunoblot, cell growth, and apoptosis data. *P* values ≤ 0.05 were considered statistically significant. The Chou-Talalay method (22) was

used to determine combination indices (CIs) for the agents. A CI value of 1 indicated an additive effect, < 1 synergism, and > 1 antagonism. The mean CI values were calculated at different effect levels (50%, 75%, and 90% effective concentrations). All statistical tests were two-sided and the results are expressed as the mean \pm standard deviation (error bars) of triplicate samples

Results

Co-targeting of signaling pathways with AZD8055 and selumetinib enhanced the growth-inhibitory effect of either agent alone in AML cells

Targeted treatment with MEK inhibitor selumetinib or the allosteric mTOR inhibitors CCI779 or RAD001 had had only limited effects in most leukemia cell lines in our previous studies (6,7). Therefore, for the current study, we assessed the effect of combining selumetinib with the novel mTOR kinase inhibitor AZD8055 in AML cell lines. Synergistic effects on cell growth inhibition were observed with OCI/AML3, U937, or MOLM13. (Fig. 1A, Supplementary Fig. S2). AML cells that displayed synergistic effects in response to the combination treatment expressed relatively high levels of p-ERK and p-AKT (Fig. 1B). However, KG-1 cells lack detectable p-ERK and p-AKT and showed an antagonistic effect. Furthermore, the combination treatment notably suppressed the levels of ERK1/2 (Thr202/Tyr204) and AKT (Ser473) phosphorylation in the OCI/AML3, MOLM13, and U937 cells but had no consistent effect on the phosphorylation of AKT Thr308 (Fig. 1C).

We next measured BrdU incorporation by flow cytometry to determine whether the combination treatment affected cell cycle progression. In all lines, cell cycle progression was modestly impaired by the single and combination agent treatments as there were fewer cells in S-phase of the cell cycle compared to the controls (Fig. 1D). Although KG-1 cells lack detectable p-AKT and express only trace levels of p-ERK, ~ 50% of these cells were apparently blocked from entering S-phase by mTOR or combined inhibition compared with controls (Fig. 1D).

The KG-1 cells expressed p-S6K (Ser240/244), which was markedly suppressed by the combination treatment (Fig. 1C), suggesting that S6 protein may be critical in the G₁-S-phase transition of the cell cycle. Interestingly, the expression of p-S6K, which is best known as a downstream target of PI3K/mTOR/AKT signaling rather than as a target of one of the MEK/ERK signaling cascades, decreased significantly when MEK signaling was suppressed by selumetinib only in OCI/AML3 and U937 cells, but not in MOLM13 or KG-1 cells. In contrast, the phosphorylation of eukaryotic initiation factor 4E-binding protein (4E-BP1), a downstream protein activated by mTORC1/S6K signaling (23), was inhibited by AZD8055 but not selumetinib in all four cell lines (Fig. 1C). Up-regulation of the cell-cycle inhibitor p27Kip-1 and down-regulation of the G₁ phase-related checkpoint protein cyclin D1/cdk4 complexes were observed in all tested AML cell lines. However, down-regulation of cdk2, cdc2, and p-Rb was generally observed in OCI/AML3, MOLM13, and U937 cells, but not in KG-1 cells, suggesting that these proteins may be not specific to the G₁-S-phase transition of the cell cycle.

Blockade of mTOR/MEK signaling has synergistic cytotoxic effects that are associated with modulation of pro-apoptotic Bim and anti-apoptotic Mcl-1 proteins

The AZD8055 and selumetinib agent combination produced synergistic pro-apoptotic effects in OCI/AML3, MOLM13, and U937 cells (Fig. 2A). In addition, in OCI/AML3, MOLM13, and U937 cells, the pro-apoptotic protein Bim was upregulated and the antiapoptotic proteins Mcl-1, p-Bad(Ser136), and survivin were downregulated by AZD8055 and even more so by the combination with selumetinib (Fig. 2B). We also observed modulated expression of the p53-regulated proteins Puma and Bad in certain leukemia cell lines. However, no notable changes in the expression of Bcl-2, Bcl-xL, or Bax were observed. Of note, the up-regulation of Bim expression and down-regulation of Mcl-1 expression correlated with cleavage of caspase-3, implying that Bim and Mcl-1 play important roles in apoptosis induction. This combination was seemingly antagonistic in the KG-1 cells (Fig. 2A), which have a low basal level of ERK and AKT activation, and did not affect Mcl-1 expression in these cells (Fig. 2B).

We therefore suspected that the modulation of Mcl-1 and Bim levels might play a key role in the combination treatment-induced apoptosis. Further investigation of the mRNA transcription level showed that the combination upregulated Bim only in MOLM13, but not in OCI/AML3 cells. No statistically significant modulation was observed in Mcl-1 levels (Fig. 2C). We next treated OCI/AML3 cells in the presence of the protein translation inhibitor cycloheximide, which further induced apoptosis in the treatment groups (Fig. 2D). Cycloheximide treatment moderately decreased protein levels of Bim, but not of Mcl-1 after 6-hour exposure. (Fig. 2D, inset). On the other hand, suppression of protein degradation with proteasome inhibitors Bortezomib or MG132 did not markedly influence the combination-induced cell apoptosis (Supplementary Fig. S3). Taken together, the combination-induced changes of Mcl-1 and Bim protein levels might result from translational, rather than transcriptional or proteasomal degradation, effects.

To further evaluate the roles of Bim and Mcl-1 in apoptosis induction, we silenced Bim expression with siRNA or Mcl-1 expression with shRNA and assessed apoptosis induction after treatment with AZD8055 and selumetinib for 48 hours. The knockdown of Bim markedly reversed the combination effect of apoptosis induction by the treatment with AZD8055 and selumetinib in OCI/AML3 (Fig. 3A) and U937 (Supplementary Fig. S4) cells, whereas the knockdown of Mcl-1 enhanced this effect in OCI/AML3 cells (Fig. 3B). These results suggested that Bim and Mcl-1 play opposite roles in apoptosis induction by this combination treatment in the AML cells.

Interference with Bcl-2 protein dimerization enhanced apoptotic effects induced by combined AZD8055 and selumetinib in AML cells

Because the induction of apoptosis in leukemia cells is largely controlled by dimerization of proapoptotic and antiapoptotic proteins (11), we hypothesized that, in addition to the inhibition of mTOR/MEK signaling, the inhibition of binding of Bax or Bim with their respective partners, Bcl-2 and Bcl-xL would further enhance apoptosis induction. We, and others, have reported previously that the Bcl-2 antagonist ABT-737 can bind to Bcl-2 family members resulting in leukemic cell death (12,24). In addition, the expression level of the

anti-apoptotic Mcl-1 protein is inversely correlated with cell sensitivity to ABT-737 due to the inability of the latter to bind and inhibit Mcl-1 (12,25). We tested the three-drug combination of ABT-737, AZD8055, and selumetinib at low concentrations (0.06, 0.1, and 0.3 $\mu\text{mol/L}$, respectively) and observed significantly enhanced proapoptotic responses in KG-1, OCI/AML3, and MOLM13 cells compared with ABT-737 only or with the AZD8055/selumetinib combination only (Fig. 4A). In the U937 cells which had the lowest basal level of Bcl-2 protein of the four AML cell lines tested (Fig. 1B), this drug combination did not induce marked apoptosis (Fig. 4A). However, apoptosis induction in the U937 cells could be boosted by increasing the concentrations of AZD8055 to 0.3 $\mu\text{mol/L}$ and selumetinib to 0.9 $\mu\text{mol/L}$ (Fig. 4B), suggesting that at higher doses of the mTOR inhibitors were still capable of inducing apoptosis in leukemic cells possessing a high basal level of p-AKT driven by PTEN deletion. Impressively, the KG-1 cells that were resistant to selumetinib and AZD8055 (Supplementary Figs. S5 and S6), demonstrated enhanced sensitivity to the three-drug combination after a 48-hour treatment (Fig. 4A).

We treated the ABT-737-sensitive KG-1 cells and ABT-737-resistant OCI/AML3 cells with ABT-737 alone or with AZD8055/selumetinib combination to gain an insight into the mechanism of apoptosis induction by the triple-drug combination treatment. An immunoprecipitation assay pull-down of the Bcl-2 complex with anti-Bcl-2 antibody indicated that Bcl-2/Bax heterodimerization was reduced in both cell lines after a 6-hour ABT-737 treatment, and even more markedly so in cells treated with all the three drugs (Fig. 4C). After a 24-hour combination treatment, we observed the cleavage of caspase-9, caspase-8, caspase-3, and Bid, cytochrome *c* release, and the localization of Bax to the mitochondria (Fig. 4D). Furthermore, Bax was upregulated resulting in an increased Bax:Bcl-2 ratio, and the expression of Mcl-1 and the X-chromosome-linked inhibitor of apoptosis protein (XIAP) were decreased possibly because of caspase-3-mediated cleavage. These findings suggested that ABT-737 enhances the proapoptotic effect of the AZD8055/selumetinib combination by interfering with Bcl-2 function thus triggering mitochondria-mediated cell death.

Three-drug combination treatment exerted synergistic proapoptotic effects in AML blast cells with *NRAS* mutations

We next tested the three-drug combination on peripheral blood or bone marrow cells obtained from AML patients (the patient cytogenetic characteristics are summarized in Supplementary Table 2). Because *RAS* mutation is known to activate both the MEK and mTOR pathways, we assessed apoptosis induction in these samples based on their *NRAS* mutational status. Selumetinib or AZD8055 alone induced modest apoptosis in five of seven samples harboring *NRAS* mutations (i.e., cases 3, 4, 5, 6 and 7) (Fig. 5A), and in one sample with wild-type *RAS* that had an *FLT3-ITD* mutation (i.e., case 11) (Fig. 5B). By comparison, the combination treatment with both agents enhanced apoptosis in most *NRAS*-mutated samples (except case 2) (Fig. 5A), and in two of the seven *NRAS*-wild-type samples (i.e., cases 11 and 13) (Fig. 5B). Both of the latter cases harbored mutations of *FLT3*. Except for cases 1 and 3, ABT-737 was highly effective in inducing apoptosis in primary AML cells, and the combination of all three agents further induced apoptosis in bulk leukemic, as well as in $\text{CD34}^+/\text{CD33}^+$ cells in 12 of 14 patient samples. Overall, the specific apoptosis

induction by the three-agent combination was higher in the CD33⁺/CD34⁺ AML progenitor cells of *NRAS* mutated AML samples compared to those with *NRAS* wild type ($p < 0.01$, Fig. 5C). These results indicate that *NRAS*-mutated AML progenitor cells might be more dependent on MEK/mTOR signaling than *NRAS* wild-type cells.

To confirm that these agents effectively blocked the corresponding signaling pathway in primary leukemia cells, we measured the p-ERK and p-AKT levels in one *NRAS* mutated AML sample (Case 7) using immunoblotting. The results indicated that targeting MEK or mTOR with the corresponding drugs or their combination markedly suppressed phosphorylation of ERK or AKT (Fig. 5D). The pattern of phosphorylation suppression of ERK/AKT correlated with apoptosis induction caused by these inhibitors (figure 5A, Case 7).

Finally, we investigated the molecular mechanisms governing apoptotic cell death in the *NRAS*-mutant AML cells. We compared the modulation of the expression of the key apoptotic and signaling proteins in isogenic-paired *NRAS*-wild-type and *NRAS*-mutated AML cells MV4-11. Compared with wild-type cells, cells with mutant *NRAS* were considerably more sensitive to treatment with selumetinib and ABT-737, or to the three-drug combination (Fig. 6A). Immunoblotting demonstrated enhanced MAPK signaling in *NRAS*-mutated cells manifesting as high basal levels of p-ERK, in concert with a high expression of Mcl-1 (Fig. 6B). However, the suppression of p-ERK with selumetinib failed to markedly suppress Mcl-1, and it triggered only a modest induction of apoptosis as shown by the level of cleaved caspase-3. In turn, the combined selumetinib and AZD8055 further diminished the level of Mcl-1 in *NRAS*-mutant cells, and this combination paired with ABT-737 caused a marked decrease of Mcl-1 protein and triggered a discernible cleavage of caspase-3 (Fig. 6B). Furthermore, at low concentrations of three inhibitors, neither ABT-737 alone nor selumetinib/AZD8055 combination triggered the loss of Ψ_m . However, ABT-737 plus selumetinib and AZD8055 showed a major Ψ_m depolarization, which was even more pronounced in the *NRAS*-mutant cells (Fig. 6C), suggesting a critical role for mitochondrial-mediated apoptosis in the triple drug combination-induced leukemia cell death, especially in the cells with *NRAS* mutations.

Discussion

In this study, we tested the combination effects of the MEK inhibitor selumetinib and the mTOR inhibitor AZD8055 in human AML cells. Simultaneous inhibition of ERK and mTOR signaling by these agents led to an enhanced cytostatic effect in the OCI/AML3, MOLM13, and U937 cells. However, this treatment showed no synergistic effect in the KG-1 cells, which exhibit only trace basal levels of phospho-ERK and -AKT. Interestingly, we noticed that targeting MEK signaling with selumetinib drastically suppressed the p-S6K level in the OCI/AML3 and U937 cells, which was not accompanied by a decrease in the level of p-4E-BP1. The S6K and 4E-BP1 proteins are well-known mTOR substrates that contribute to cell proliferation and survival (26). S6K modulation by MAPK signaling is not well understood, although the PI3K/Akt and Ras/MAPK pathways are known to signal in a parallel manner to regulate Tsc1 and 2, and mediate the phosphorylation of S6K (27). Our data indicate that MEK/ERK signaling in conjunction with mTOR signaling plays a

prominent role in regulating S6K activity in AML cells. However, the blockade of S6K activity alone is not the major predictor of cell sensitivity to MEK inhibition as exemplified by the vastly different mean half maximal inhibitory concentrations required for inhibiting the growth of OCI/AML3 cells (0.03 $\mu\text{mol/L}$, 95% CI: 0.01 to 0.08 $\mu\text{mol/L}$) and U937 cells (392 $\mu\text{mol/L}$, 95% CI: 0.5 to 2960 $\mu\text{mol/L}$) (Supplementary Fig. S5) despite a similar suppression level of p-S6K. Conversely, mTOR inhibition not only activated MAPK signaling, which is reportedly dependent on a feedback loop of the S6K/PI3K/Ras pathway (14), but it also relieves the negative feedback loop resulting in increased phosphorylation of AKT at Thr308 (28). Our findings support the notion that multiple circuitry feedback mechanisms are operational in these cells, and may also explain, at least in part, why the blockade of the AKT/mTOR/S6K axis had limited activity in phase I/II clinical trials in patients with hematological malignancies (29).

The interaction and balance between pro- and anti-apoptotic Bcl2 family proteins dictates cell fate (30). Bim is a positive effector of apoptosis induction and is involved in mitochondria-mediated apoptosis induction (31). Our previous studies demonstrated that up-regulation of Bim expression, which triggers mitochondria-mediated apoptosis, plays a critical role in the anti-leukemia efficacy of Raf/MEK/ERK inhibitors (32). In the present study, we showed that selumetinib, or both selumetinib and AZD8055, markedly up-regulated Bim expression, and that the further addition of ABT-737 enhanced this up-regulation as well as apoptosis induction. In contrast, silencing the expression of Bim markedly diminished apoptosis induction by the agents.

The level of Mcl-1 is a predictive biomarker for sensitivity to therapy-induced apoptosis induction in a variety of hematopoietic malignancies, and its upregulation was mediated via ERK/Elk-1 or AKT/mTOR signaling (33,34). Consistent with these reported findings, targeting of MEK or mTOR decreased Mcl-1 expression. Mcl-1 expression was further diminished in the presence of ABT-737 and resulted in enhanced apoptosis induction in AML cells. Moreover, lowering the Mcl-1 level by shRNA enhanced drug-induced apoptosis (Supplementary Fig. S7). Specifically, compared with *NRAS*-wild-type MV4-11 cells, the *NRAS*-mutant MV4-11 cells expressed a higher basal level of Mcl-1 protein that was subsequently diminished by the combined targeting of MEK, mTOR, and Bcl-2 pathways to trigger apoptosis induction. Thus, the three-drug combination was much more effective against AML cells with *NRAS* mutations compared to those with wild-type *NRAS*.

The interaction of Bim with Mcl-1 interferes with the cytochrome *c*-releasing capability of Bim and protects cells against Bim-mediated apoptosis (35). The down-regulation of Mcl-1 expression (or cleavage of Mcl-1) may lead to release of Bim from specific binding with Mcl-1 to trigger apoptosis. ERK-mediated phosphorylation of Bim EL (i.e., the extra-long spliced form of the Bim protein) promotes its proteasomal degradation (36), and phosphorylation of Mcl-1 slows this turnover (37). Furthermore, Akt-dependent glucose metabolism and ERK/ELK-1 activation promote Mcl-1 synthesis to maintain cell survival and differentiation (38,39). Our findings suggest that the simultaneous suppression of PI3K/mTOR signaling and interference with Bcl-2 family protein dimerization are essential for drug-induced death of AML cells with a high AKT expression. A recent study using U937 cells indicated that the combination of PI3K/mTOR inhibitors with ABT-737 abrogated Bim

binding to Bcl-2/Bcl-xL, which allowed Bim to activate Bax and Bak to exert pro-apoptotic activity (40). Recent studies indicate that leukemia stem cells (LSCs) are characterized by relatively low levels of reactive oxygen species with an aberrant overexpression of BCL-2. Interestingly, the inhibition of BCL-2 reduced oxidative phosphorylation and selectively eradicated these quiescent LSCs (41). In our study, AML cells with high p-AKT and p-ERK levels (e.g., the MV4-11-NRAS-mutated cells) were efficiently killed by the triple-drug combination. This was accompanied by loss of Ψ_m indicating the high anti-leukemia potency of this treatment strategy against AML cells with gain-of-function NRAS mutations. This would also suggest a selective potency of this combination for targeting quiescent LSCs.

In summary, co-targeting the MEK and mTOR pathways may be an effective treatment strategy for patients who have AML cells that express high levels of MEK and mTOR, or in patients whose AML cells harbor NRAS mutations. This treatment may be further potentiated using the BH3 mimetic ABT-737. This three-drug combination could pave the way for the development of integrated therapeutic strategies that take advantage of the synergistic anti-leukemia effects thereby leading to the design of novel, clinically viable combinations for AML therapy.

Supplementary Material

Refer to Web version on PubMed Central for supplementary material.

Acknowledgments

We thank Wenjing Chen and Teresa McQueen who provided patient information and prepared patient samples for this study, AstraZeneca for providing selumetinib and AZD8055, and Numsen Hail, Jr. and Elizabeth L. Hess who provided critical reviews and editorial assistance to the authors during preparation of this manuscript.

Grant Support: This work was supported in part by grants from NIH/NCI (CA143805, CA100632, CA055164, and CA049639) and a Cancer Center Support Grant (CA 16672) (to M.A.), and a Leukemia SPORE Career Development Award (CA100632-05) (to W.Z.).

References

1. Bacher U, Haferlach T, Schoch C, Kern W, Schnittger S. Implications of NRAS mutations in AML: a study of 2502 patients. *Blood*. 2006; 107:3847–53. [PubMed: 16434492]
2. Illmer T, Thiede C, Fredersdorf A, Stadler S, Neubauer A, Ehninger G, et al. Activation of the RAS pathway is predictive for a chemosensitive phenotype of acute myelogenous leukemia blasts. *Clin Cancer Res*. 2005; 11:3217–24. [PubMed: 15867216]
3. Altman JK, Plataniias LC. Prospects for mTOR targeting in adult T cell leukemia. *Leuk Lymphoma*. 2009; 50:525–6. [PubMed: 19373648]
4. Kornblau SM, Womble M, Qiu YH, Jackson CE, Chen W, Konopleva M, et al. Simultaneous activation of multiple signal transduction pathways confers poor prognosis in acute myelogenous leukemia. *Blood*. 2006; 108:2358–65. [PubMed: 16763210]
5. Milella M, Kornblau SM, Estrov Z, Carter BZ, Lapillonne H, Harris D, et al. Therapeutic targeting of the MEK/MAPK signal transduction module in acute myeloid leukemia. *J Clin Invest*. 2001; 108:851–9. [PubMed: 11560954]
6. Zeng Z, Sarbassov dD, Samudio IJ, Yee KW, Munsell MF, Ellen JC, et al. Rapamycin derivatives reduce mTORC2 signaling and inhibit AKT activation in AML. *Blood*. 2007; 109:3509–12. [PubMed: 17179228]

7. Zhang W, Konopleva M, Burks JK, Dywer KC, Schober WD, Yang JY, et al. Blockade of mitogen-activated protein kinase/extracellular signal-regulated kinase kinase and murine double minute synergistically induces Apoptosis in acute myeloid leukemia via BH3-only proteins Puma and Bim. *Cancer Res.* 2010; 70:2424–34. [PubMed: 20215498]
8. Yuan R, Kay A, Berg WJ, Leibold D. Targeting tumorigenesis: development and use of mTOR inhibitors in cancer therapy. *J Hematol Oncol.* 2009; 2:45. [PubMed: 19860903]
9. Milella M, Kornblau SM, Andreeff M. The mitogen-activated protein kinase signaling module as a therapeutic target in hematologic malignancies. *Rev Clin Exp Hematol.* 2003; 7:160–90. [PubMed: 14763161]
10. Karakas T, Maurer U, Weidmann E, Miething CC, Hoelzer D, Bergmann L. High expression of bcl-2 mRNA as a determinant of poor prognosis in acute myeloid leukemia. *Ann Oncol.* 1998; 9:159–65. [PubMed: 9553660]
11. Samudio I, Konopleva M, Carter B, Andreeff M. Apoptosis in leukemias: regulation and therapeutic targeting. *Cancer Treat Res.* 2010; 145:197–217. [PubMed: 20306253]
12. Konopleva M, Contractor R, Tsao T, Samudio I, Ruvolo PP, Kitada S, et al. Mechanisms of apoptosis sensitivity and resistance to the BH3 mimetic ABT-737 in acute myeloid leukemia. *Cancer Cell.* 2006; 10:375–88. [PubMed: 17097560]
13. Roberts AW, Seymour JF, Brown JR, Wierda WG, Kipps TJ, Khaw SL, et al. Substantial susceptibility of chronic lymphocytic leukemia to BCL2 inhibition: results of a phase I study of navitoclax in patients with relapsed or refractory disease. *J Clin Oncol.* 2012; 30:488–96. [PubMed: 22184378]
14. Carracedo A, Ma L, Teruya-Feldstein J, Rojo F, Salmena L, Alimonti A, et al. Inhibition of mTORC1 leads to MAPK pathway activation through a PI3K-dependent feedback loop in human cancer. *J Clin Invest.* 2008; 118:3065–74. [PubMed: 18725988]
15. Oltsersdorf T, Elmore SW, Shoemaker AR, Armstrong RC, Augeri DJ, Belli BA, et al. An inhibitor of Bcl-2 family proteins induces regression of solid tumours. *Nature.* 2005; 435:677–81. [PubMed: 15902208]
16. Clodi K, Kliche K-O, Zhao S, Weidner D, Schenk T, Consoli U, et al. Cell-surface exposure of phosphatidylserine correlates with the stage of fludarabine-induced apoptosis in chronic lymphocytic leukemia (CLL) and expression of apoptosis-regulating genes. *Cytometry.* 2000; 40:19–25. [PubMed: 10754513]
17. ten Cati B, Samplonius DF, Bijma T, de Leij LF, Helfrich W, Bremer E. The histone deacetylase inhibitor valproic acid potently augments gemtuzumab ozogamicin-induced apoptosis in acute myeloid leukemic cells. *Leukemia.* 2007; 21:248–52. [PubMed: 17122863]
18. Zhang W, McQueen T, Schober W, Rassidakis G, Andreeff M, Konopleva M. Leukotriene B4 receptor inhibitor LY293111 induces cell cycle arrest and apoptosis in human anaplastic large-cell lymphoma cells via JNK phosphorylation. *Leukemia.* 2005; 19:1977–84. [PubMed: 16151469]
19. Ruvolo PP, Zhou L, Watt JC, Ruvolo VR, Burks JK, Jiffar T, et al. Targeting PKC-mediated signal transduction pathways using enzastaurin to promote apoptosis in acute myeloid leukemia-derived cell lines and blast cells. *J Cell Biochem.* 2011; 112:1696–707. [PubMed: 21360576]
20. Ruvolo VR, Karanjeet KB, Schuster TF, Brown R, Deng Y, Hinchcliffe E, et al. Role for PKC delta in Fenretinide-Mediated Apoptosis in Lymphoid Leukemia Cells. *J Signal Transduct.* 2010; 2010:584657. [PubMed: 20844597]
21. Poot M, Pierce RH. Detection of changes in mitochondrial function during apoptosis by simultaneous staining with multiple fluorescent dyes and correlated multiparameter flow cytometry. *Cytometry.* 1999; 35:311–7. [PubMed: 10213196]
22. Chou TC. Drug combination studies and their synergy quantification using the Chou-Talalay method. *Cancer Res.* 2010; 70:440–6. [PubMed: 20068163]
23. Kim DH, Sabatini DM. Raptor and mTOR: subunits of a nutrient-sensitive complex. *Curr Top Microbiol Immunol.* 2004; 279:259–70. [PubMed: 14560962]
24. Konopleva M, Milella M, Ruvolo P, Watts JC, Ricciardi MR, Korchin B, et al. MEK inhibition enhances ABT-737-induced leukemia cell apoptosis via prevention of ERK-activated MCL-1 induction and modulation of MCL-1/BIM complex. *Leukemia.* 2012; 26:778–87. [PubMed: 22064351]

25. van Delft MF, Wei AH, Mason KD, Vandenberg CJ, Chen L, Czabotar PE, et al. The BH3 mimetic ABT-737 targets selective Bcl-2 proteins and efficiently induces apoptosis via Bak/Bax if Mcl-1 is neutralized. *Cancer Cell*. 2006; 10:389–99. [PubMed: 17097561]
26. Meyuhas O, Dreazen A. Ribosomal protein S6 kinase from TOP mRNAs to cell size. *Prog Mol Biol Transl Sci*. 2009; 90:109–53. [PubMed: 20374740]
27. Ma L, Chen Z, Erdjument-Bromage H, Tempst P, Pandolfi PP. Phosphorylation and functional inactivation of TSC2 by Erk implications for tuberous sclerosis and cancer pathogenesis. *Cell*. 2005; 121:179–93. [PubMed: 15851026]
28. Das F, Ghosh-Choudhury N, Dey N, Mandal CC, Mahimainathan L, Kasinath BS, et al. Unrestrained mammalian target of rapamycin complexes 1 and 2 increase expression of phosphatase and tensin homolog deleted on chromosome 10 to regulate phosphorylation of Akt kinase. *J Biol Chem*. 2012; 287:3808–22. [PubMed: 22184110]
29. Yee KW, Zeng Z, Konopleva M, Verstovsek S, Ravandi F, Ferrajoli A, et al. Phase I/II study of the mammalian target of rapamycin inhibitor everolimus (RAD001) in patients with relapsed or refractory hematologic malignancies. *Clin Cancer Res*. 2006; 12:5165–73. [PubMed: 16951235]
30. Adams JM, Cory S. The Bcl-2 apoptotic switch in cancer development and therapy. *Oncogene*. 2007; 26:1324–37. [PubMed: 17322918]
31. Bouillet P, Metcalf D, Huang DC, Tarlinton DM, Kay TW, Kontgen F, et al. Proapoptotic Bcl-2 relative Bim required for certain apoptotic responses, leukocyte homeostasis, and to preclude autoimmunity. *Science*. 1999; 286:1735–8. [PubMed: 10576740]
32. Zhang W, Konopleva M, Ruvolo VR, McQueen T, Evans RL, Bornmann WG, et al. Sorafenib induces apoptosis of AML cells via Bim-mediated activation of the intrinsic apoptotic pathway. *Leukemia*. 2008; 22:808–18. [PubMed: 18200035]
33. Booy EP, Henson ES, Gibson SB. Epidermal growth factor regulates Mcl-1 expression through the MAPK-Elk-1 signalling pathway contributing to cell survival in breast cancer. *Oncogene*. 2011; 30:2367–78. [PubMed: 21258408]
34. Mills JR, Hippo Y, Robert F, Chen SM, Malina A, Lin CJ, et al. mTORC1 promotes survival through translational control of Mcl-1. *Proc Natl Acad Sci U S A*. 2008; 105:10853–8. [PubMed: 18664580]
35. Han J, Goldstein LA, Gastman BR, Froelich CJ, Yin XM, Rabinowich H. Degradation of Mcl-1 by granzyme B: implications for Bim-mediated mitochondrial apoptotic events. *J Biol Chem*. 2004; 279:22020–9. [PubMed: 15014070]
36. Luciano F, Jacquet A, Colosetti P, Herrant M, Cagnol S, Pages G, et al. Phosphorylation of Bim-EL by Erk1/2 on serine 69 promotes its degradation via the proteasome pathway and regulates its proapoptotic function. *Oncogene*. 2003; 22:6785–93. [PubMed: 14555991]
37. Domina AM, Vrana JA, Gregory MA, Hann SR, Craig RW. MCL1 is phosphorylated in the PEST region and stabilized upon ERK activation in viable cells, and at additional sites with cytotoxic okadaic acid or taxol. *Oncogene*. 2004; 23:5301–15. [PubMed: 15241487]
38. Coloff JL, Macintyre AN, Nichols AG, Liu T, Gallo CA, Plas DR, et al. Akt-dependent glucose metabolism promotes Mcl-1 synthesis to maintain cell survival and resistance to Bcl-2 inhibition. *Cancer Res*. 2011; 71:5204–13. [PubMed: 21670080]
39. Townsend KJ, Zhou P, Qian L, Bieszcza CK, Lowrey CH, Yen A, et al. Regulation of MCL1 through a serum response factor/Elk-1-mediated mechanism links expression of a viability-promoting member of the BCL2 family to the induction of hematopoietic cell differentiation. *J Biol Chem*. 1999; 274:1801–13. [PubMed: 9880563]
40. Rahmani M, Aust MM, Attkisson E, Williams DC Jr, Ferreira-Gonzalez A, Grant S. Dual inhibition of Bcl-2 and Bcl-xL strikingly enhances PI3K inhibition-induced apoptosis in human myeloid leukemia cells through a. *Cancer Res*. 2013; 73:1340–51. [PubMed: 23243017]
41. Lagadinou ED, Sach A, Callahan K, Rossi RM, Neering SJ, Minhajuddin M, et al. BCL-2 inhibition targets oxidative phosphorylation and selectively eradicates quiescent human leukemia stem cells. *Cell Stem Cell*. 2013; 12:329–41. [PubMed: 23333149]

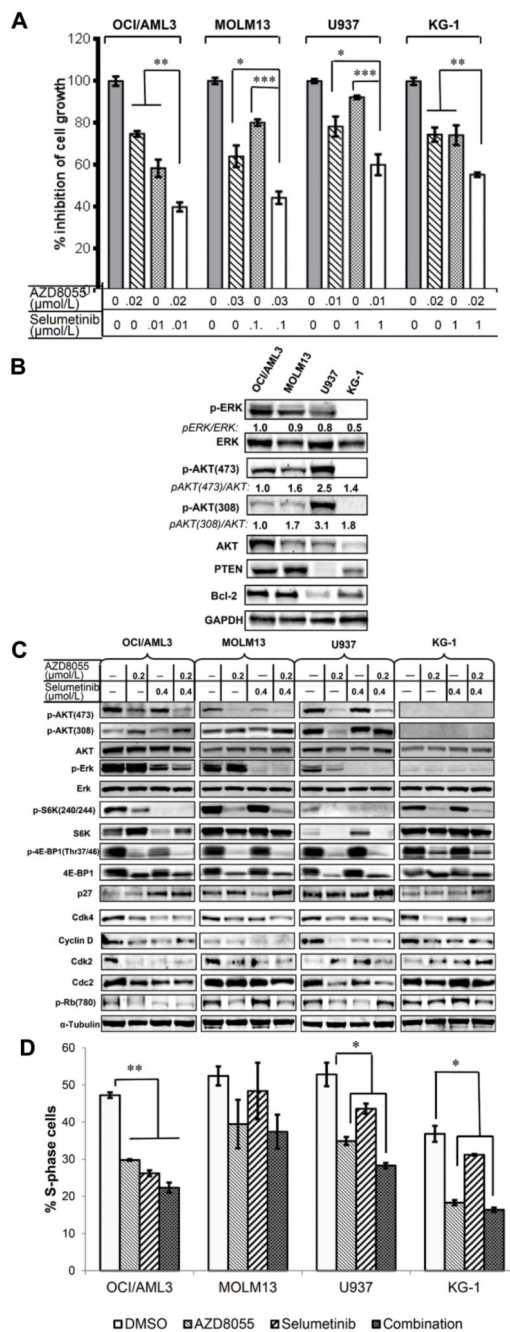
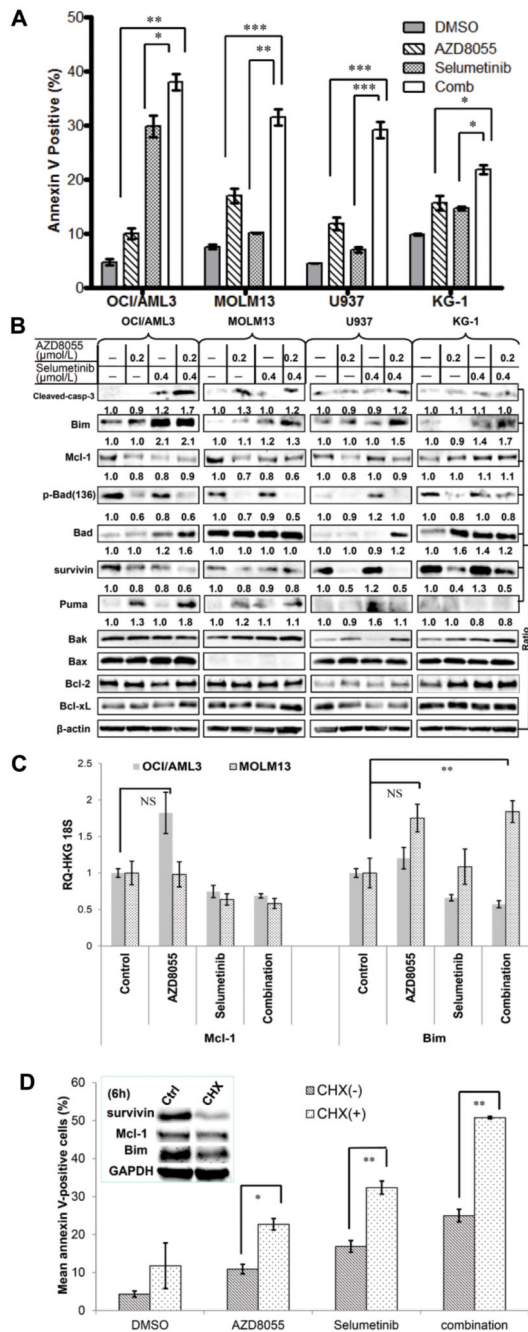


Figure 1.

Dual blockade of mTOR/MEK signaling synergistically or additively inhibits growth in AML lines OCI/AML3, MOLM13, and U937 but not KG-1. A, AML cells were treated with AZD8055, selumetinib, or both at the indicated concentrations for 48 hours. Inhibition of cell growth was measured using viable cell counts as described in Materials and Methods and expressed as the percentage of untreated cells. Data shown represent the mean of four independent determinations. Error bars correspond to 95% confidence intervals. * $P < 0.05$; ** $P < 0.01$. B, Basal expression levels of phosphorylated and total ERK, AKT and Bcl-2

proteins was determined by immunoblotting. Numbers indicate ratio of phosphorylated proteins to the respective total proteins. C, AML cells were treated with AZD8055 and selumetinib at the indicated concentrations for 24 hours, and the profile of signaling and cell-cycle-related checkpoint proteins was measured by immunoblotting. α -tubulin was used as loading control. D, AML cells were treated with the indicated agents for 24 hours, and BrdU incorporation was determined using flow cytometry after labeling with anti-BrdU-fluorescein isothiocyanate antibody. Data represent the mean of triplicated experiments. DMSO, dimethyl sulfoxide control.

**Figure 2.**

Synergistic proapoptotic effects induced by blockade of mTOR/MEK signaling are associated with modulation of Mcl-1 and Bim. A, AML cells were treated with AZD8055 (0.3 μmol/L), selumetinib (0.9 μmol/L), or both for 72 hours, and the percentage of apoptotic cells was determined using flow cytometry. B, Bcl-2 family proteins were assessed by immunoblotting after 24 hours of treatment with AZD8055 and selumetinib. The numbers below the blots indicate the ratio of protein to the loading control β-actin. C, OCI/AML3 and MOLM13 cells were treated with indicated inhibitors for 6 hours, and relative mRNA

expression levels were determined by real-time PCR by calculating the ratios of Mcl-1/Bim to 18S mRNA. D, OCI/AML3 cells were treated for 48 hours in the presence or absence of cycloheximide (0.5 $\mu\text{mol/L}$), and apoptosis was determined by flow cytometry. Inset: protein levels of Survivin, Mcl-1, and Bim after treatment of OCI/AML3 cells with cycloheximide (CHX) for 6 hours. * $P < 0.05$; ** $P < 0.01$; *** $P < 0.001$; NS; no statistical significance.

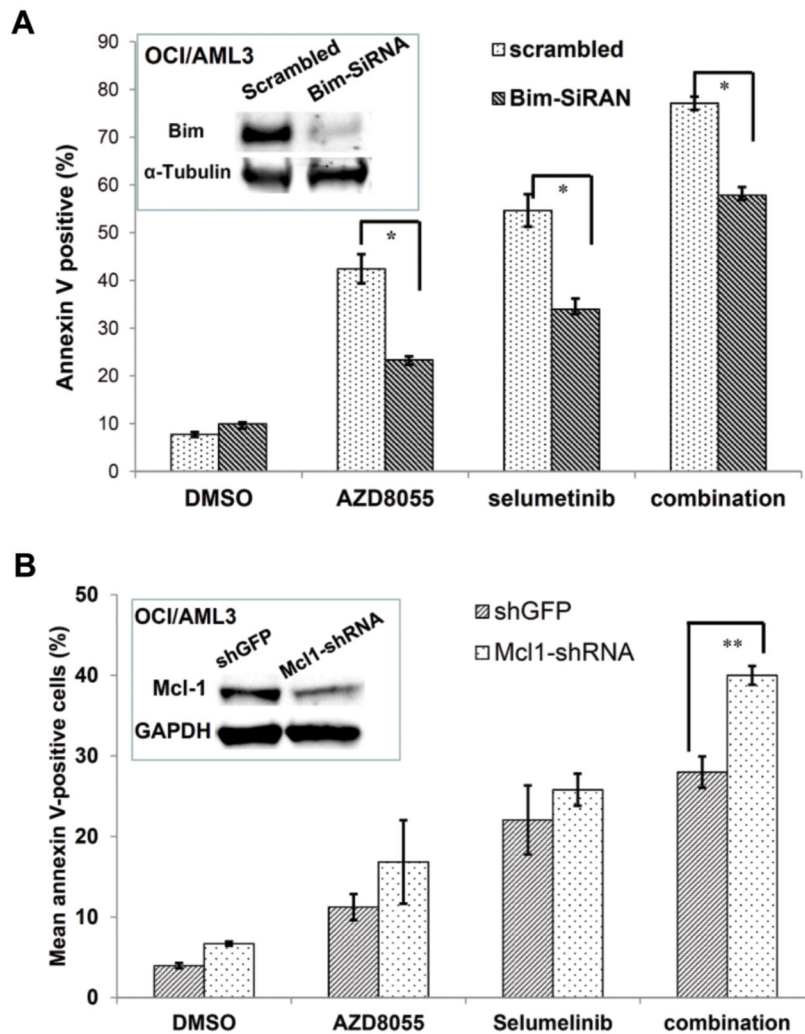
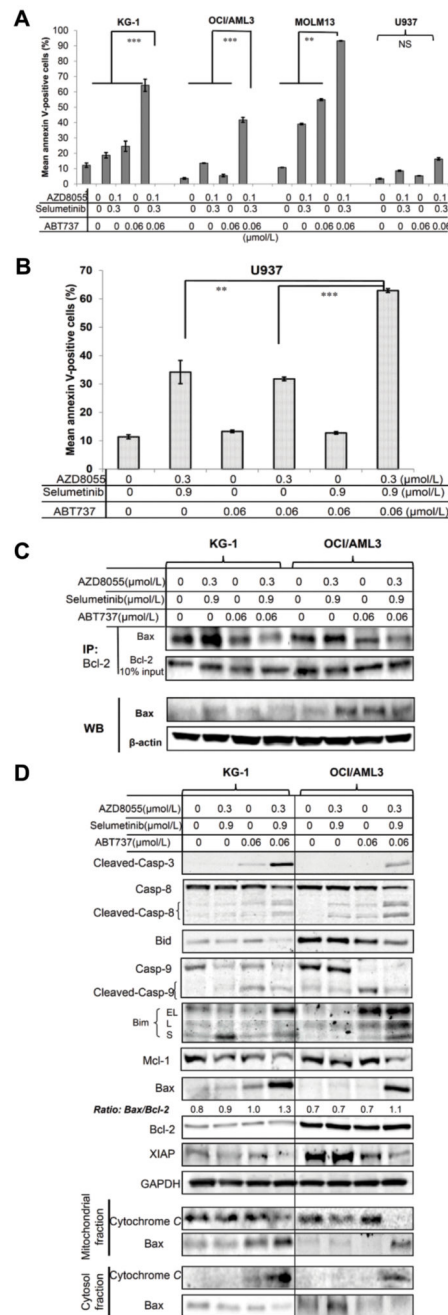


Figure 3. Levels of proapoptotic BH3-only Bim protein and antiapoptotic Mcl-1 protein play a critical role in drug combination-induced apoptosis. A, OCI/AML3 cells were electroporated with Bim siRNA or scrambled siRNA for 24 hours, treated with AZD8055 (0.4 μ mol/L) and/or selumetinib (0.2 μ mol/L) for 48 hours, and examined for apoptosis induction. Inset: knockdown of basal level of Bim protein expression. B, OCI/AML3 cells were transfected with Mcl-1 shRNA or shGFP control lentiviral vectors, the puromycin-selected cells were treated with AZD8055 (0.4 μ mol/L) and/or selumetinib (0.4 μ mol/L) for 48 hours, and examined for apoptosis induction. Inset: knockdown of basal level of Mcl-1 after puromycin selection. DMSO, dimethyl sulfoxide, control. ** $P < 0.01$.

**Figure 4.**

ABT-737 further enhances the pro-apoptotic effect of the AZD8055/selumetinib combination treatment in AML cells. A, AML cells were treated with AZD8055, selumetinib, ABT-737, or the indicated combinations for 48 hours, and examined for apoptosis induction. B, U937 cells were treated as described above and examined for apoptosis induction. ** $P < 0.01$; *** $P < 0.001$. C, KG-1 and OCI/AML3 cells were treated with ABT-737, AZD8055 plus selumetinib, or both at the indicated concentrations (in μmol/L) for 6 hours, and Bcl-2 protein was pulled down with anti-Bcl-2 antibody-

conjugated A/G beads. Bcl-2-binding Bax protein expression was measured using immunoblotting. A 10% Bcl-2 input of immunoprecipitated fractions is shown as a loading control for Bcl-2 protein level. IP, immunoprecipitation; WB, immunoblot. D, KG-1 and OCI/AML3 cells were treated with ABT-737, AZD8055 plus selumetinib, or both for 24 hours, and the cells were lysed to assess expression of apoptosis-related Bcl-2 family members in mitochondrial, cytosol, and whole-cell fractions via immunoblotting. Casp, caspase; EL, extra-long; L, long and S, short.

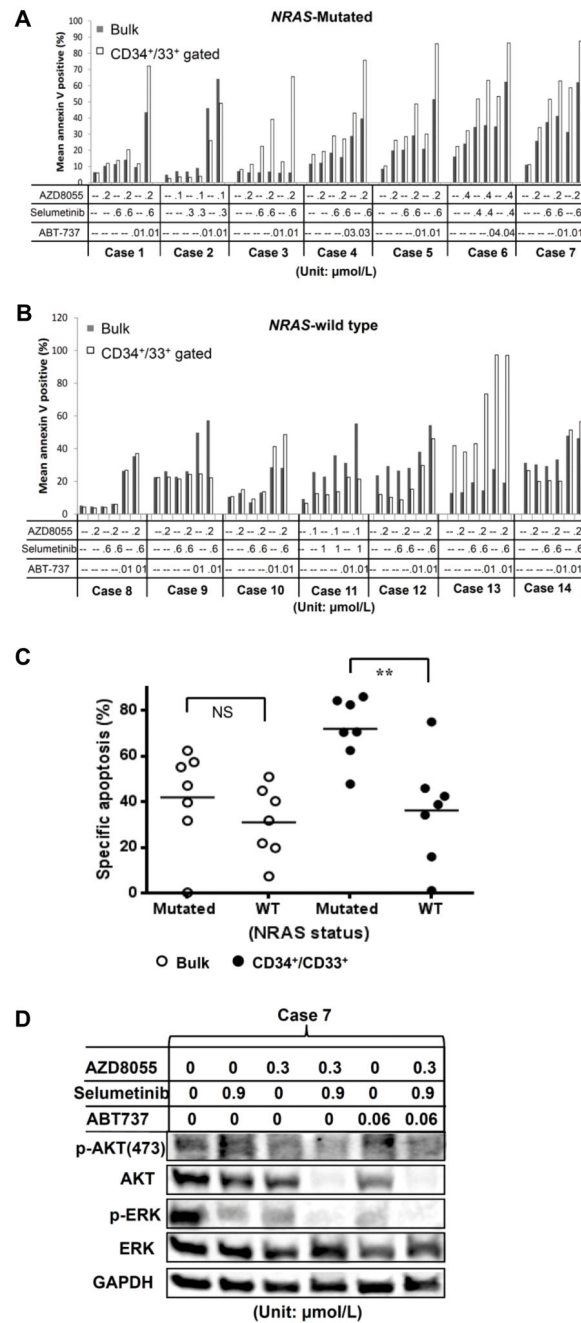
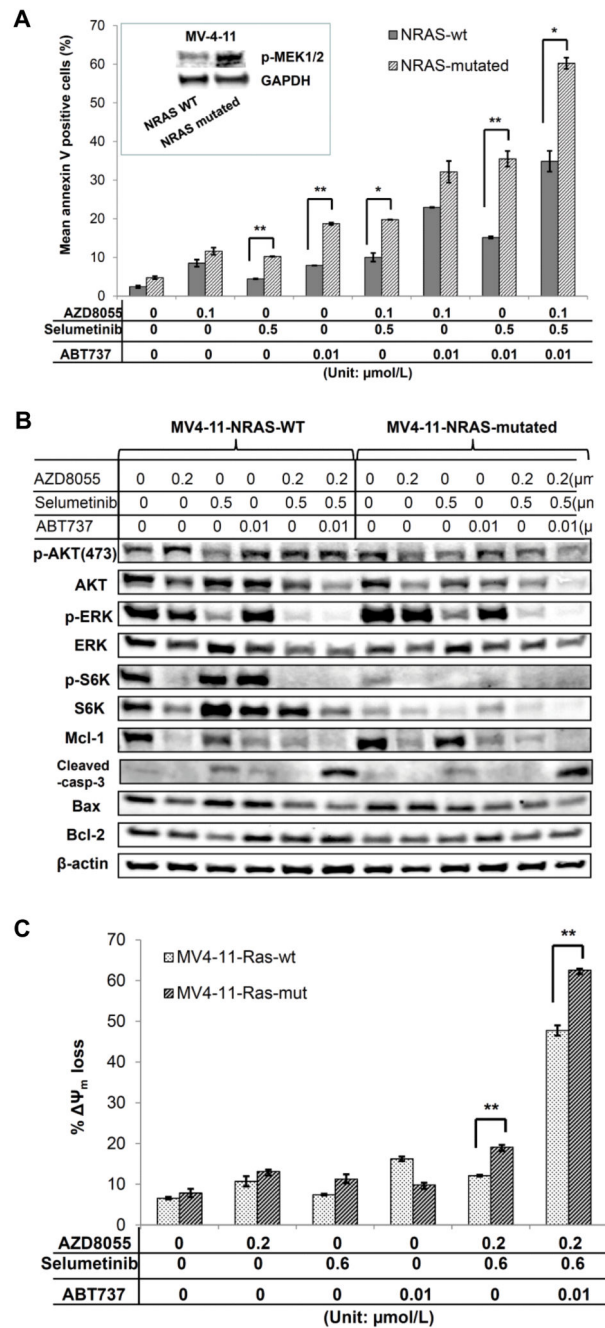


Figure 5.

Three-drug combination treatment exerts synergistic proapoptotic effects in AML blasts with *NRAS* mutations. Mononuclear cells obtained from peripheral blood and bone marrow samples of AML patients with (A) or without (B) *NRAS* mutations were exposed to AZD8055, selumetinib, and/or ABT737 at the indicated concentrations (in $\mu\text{mol/L}$) for 24 to 72 hours. C, The specific apoptosis was determined in triplicate samples based on the triple-drug treatment data shown in Fig. 5A and 5B, and shown as a comparison between bulk and CD33⁺/34⁺ fractions of the *NRAS* mutated and *NRAS*-wild samples. ** $P < 0.01$. D, AML

patient sample (case 7) was treated with indicated concentration ($\mu\text{mol/L}$) of inhibitors for 24 hours, and correlative protein expression was determined by immunoblotting.

**Figure 6.**

Mutated *NRAS* in AML cells are sensitive to selumetinib-induced apoptosis in the presence of ABT-737. A, MV4-11 cells with or without *NRAS* mutation were treated with AZD8055, selumetinib, or ABT-737, their combinations at the indicated concentrations ($\mu\text{mol/L}$) for 48 hours, and examined for apoptosis induction. Inset: basal phosphorylation level of p-MEK in wild-type (WT) and *NRAS*-mutated MV4-11 cells. * $P < 0.05$; ** $P < 0.01$. B, *NRAS*-wild type, and *NRAS*-mutant MV4-11 cells were treated with the indicated drugs ($\mu\text{mol/L}$) for 16 hours, and corresponding protein expression was measured by immunoblotting. C, *NRAS*-

WT and Ψ_m -mutated MV4-11 cells were treated with the indicated drugs ($\mu\text{mol/L}$) for 24 hours, and loss of Ψ_m was evaluated using flow cytometry after staining with CMXRos and MitoTracker Green. ** $P < 0.01$.